Progress In Electromagnetics Research B, Vol. 57, 127–138, 2014

Embedded Antenna for Metallic Handheld Communication Devices

Sangjin Eom[1, 2, *], Hosaeng Kim[2], Maifuz Ali[1], and Seong-Ook Park[1]

Abstract—In this study, a quad-band folded slot antenna with a monopole feed line embedded in a conductive housing structure (the LCD bracket of a mobile phone) is proposed. The performance of the proposed antenna is evaluated through simulation and measurement, demonstrating that it can provide total radiation efficiencies of more than 40% in the EGSM900, DCS, PCS, and WCDMA1 bands. Over these four bands, the total radiated power (TRP) of a prototype mobile phone using the antenna is 28.5, 27.1, 27.5, and 21 dBm, respectively, while the total isotropic sensitivity (TIS) is 102.7, 104.3, 103.8, and 107.3 dBm, respectively; all of these values satisfy Cellular Telecommunication and Internet Association (CTIA) requirements for over-the-area-(OTA) testing standards. The radiation performance of the proposed antenna in the calling mode is tested and shown to be within satisfactory limits; similarly, the specific absorption rates (SARs) of the prototype mobile phone are also found to be within standard SAR limits.

1. INTRODUCTION

The rapid growth in mobile communication services has created an increasing demand for ultra-small multiband and broadband internal antennas for hand-held devices. In pursuit of this goal, many planar inverted F antenna (PIFA) and mono-pole antenna designs have been developed for use in mobile phones [1]; however, neither of these designs can guarantee sufficient radiation performance for general mobile phone use when antenna reception is blocked by conductive housing in the ground plane. Conductive blocking structures and other components adjoining an antenna significantly degrade radiation performance because such components serve as EM field scatterers and create unwanted parasitic inductance and capacitance. To avoid this problem, slim and compact device configurations have begun to incorporate antennas that are more compatible with metal enclosure [2–7]. Most such designs feature a loop, slot, or an open slit antenna that utilizes the metal enclosure as a radiator component. In order to enhance device embedding, Lin et al. [8–10] and [11] investigated hybrid designs combined with slot antennas and PCB embedded planar antennas, although the resulting antennas are too large to fit into mobile phones unless the layout of nearby components such as the speaker, microphone, vibrator, and micro-USB is properly considered. In this study, we present a novel slot antenna design in which a monopole feed line is embedded into the metal ground plane or the LCD bracket. The performance of the proposed antenna in a simple real-life prototype phone is evaluated through simulation and experiment.

2. ANTENNA DESIGN

2.1. Folded Slot Antenna

Generally, slot antennas are half-wavelength electric devices that use the first resonant frequency. The physical length of a slot antenna will be determined by its operating frequency and by the materials

Received 11 October 2013, Accepted 18 November 2013, Scheduled 3 December 2013

* Corresponding author: Sangjin Eom (gabyull@kaist.ac.kr).

[1] KAIST (Korea Advanced Institute of Science and Technology), 291 Daehak-ro (373-1 Guseong-dong), Yuseong-gu, Daejeon 305-701, Republic of Korea. [2] Samsung Electronics Co., Ltd., Maetan-dong 129, Samsung-ro, Yeongtong-gu, Suwon-si, Gyeonggi-do 443-742, Republic of Korea.

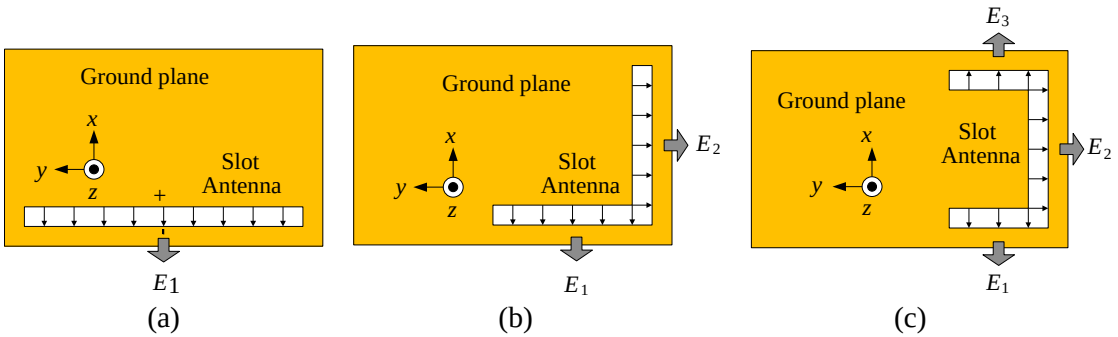

Figure 1. Slot antennas in mobile phone ground plane. (a) I-shaped slot antenna. (b) L-shaped slot antenna. (c) U-shaped slot antenna.

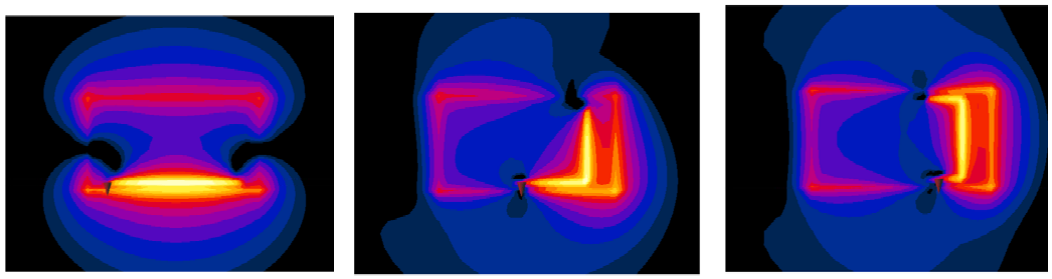

Figure 2. *E*-field distributions of the slot antennas with finite ground plane at their first resonances. (a) I-shaped slot antenna. (b) L-shaped slot antenna. (c) U-shaped slot antenna.

surrounding the slot; in absence of any surrounding high permittivity material, a slot antenna for the center frequency of the EGSM900 band (925 MHz) will be approximately 160 mm long. However, as mobile phones are usually shorter than 160 mm (generally, a mobile phone with a 3.5 $\sim$ 4.5 inches LCD will be smaller than 130 mm $\times$ 70 mm) they cannot accommodate conventional I-shaped slot antennas and instead require bent antennas. Figure 1 compares the layout of a common I-shaped slot antenna with those of two bent slot antennas that can fit into a typical mobile phone.

Slot antenna radiation performance depends on the shape of the slot, the shape and size of the ground plane, and on the matching elements and supporting materials. In this section, the radiation performances of three different slot antenna shapes on a finite ground plane with a length and width of 130 and 70 mm, respectively, are compared in order to determine a suitable mobile phone slot shape. For the purposes of this simulation, a finite ground plane mounted on an FR4 substrate with a thickness of 1 mm, a relative permittivity of 4.4, and a dielectric loss tangent of 0.02 is used in conjunction with a directly fed 110 mm $\times$ 2 mm slot antenna.

Figure 1 shows the directions of the electric fields within the slots at the first resonant frequency. In the U-shaped slot shown in Figure 1(c), *E*-field E_1 is likely to cancel out *E*-field E_3, and this would decrease radiation efficiency; however, in the real case of a finite ground, with an adequate distance between E_1 and E_3, the ground plane itself acts as a radiator, which mitigates this concern, as shown in Figure 3(b).

The electrical field distributions of an I-, L-, and U-shaped slot antenna on a finite ground plane are shown in Figure 2, from which it can be seen that both the ground plane and the slot radiate in all three cases. Specifically, Figures 2(b) and 2(c) show that L- and U-shaped slots in the limited mobile phone ground induce multi-directional radiation, unlike the I-shaped slot in Figure 2(a).

Figure 3 shows the return losses and total radiation efficiencies with direct feed for the three slot antenna types. The lengths of the L- and U-shaped slots have been optimized to allow them to resonate at the first resonance frequency of the I-shaped slot. From the figure, it can be seen that both the L- and U-shaped antennas have a wider bandwidth than the I-shaped antenna because the former antennas have a larger variety of current paths. Additionally, as shown in Figure 4, the bent-slot antennas

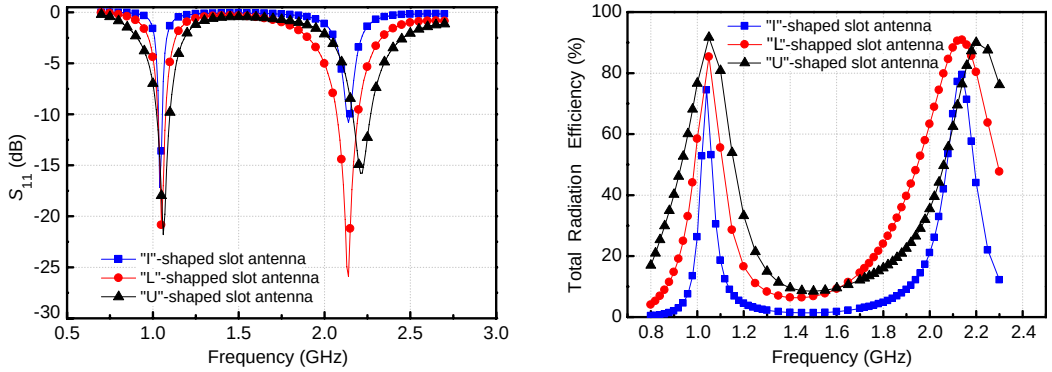

Figure 3. Radiation performance of the three slot antennas. (a) Return loss. (b) Total radiation efficiencies.

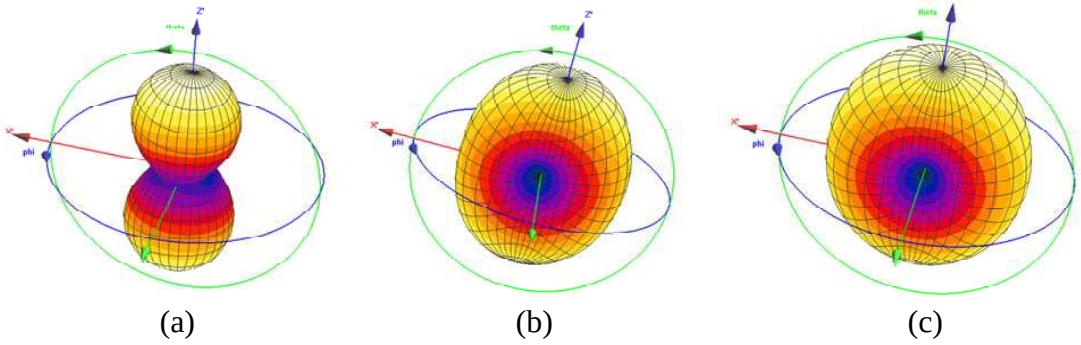

Figure 4. Three-dimensional radiation patterns. (a) I-shaped slot antenna. (b) L-shaped slot antenna. (c) U-shaped slot antenna.

radiate more omni-directionally than does the I-shaped antenna, with the U-shaped antenna displaying the most omni-directional pattern as well as the best radiation performance of the three. However, as metallic components — such as flexible cables and a micro-performance USB — that significantly reduce radiation performance must be placed across the slot, a U-shaped slot antenna is not the best choice for mobile phone use. Although the L-shaped antenna has worse radiation performance than the U-shaped antenna, it can be used more easily in actual mobile phone designs containing a variety of metal structure and components.

2.2. Proposed Slot Antenna

Based on the analysis above, we propose an L-shaped slot antenna for use in mobile phones. Figure 5 shows a detailed configuration of an antenna to be embedded into the LCD metal bracket of a mobile phone using the conductive housing structure. The proposed antenna consists primarily of two parts: an L-shaped slot and an L-shaped monopole feed line that significantly improve the antenna impedance matching in the higher bands. As the slot antenna is itself highly inductive, it cannot easily obtain wideband characteristics without matching elements, and therefore, the capacitively coupled monopole feeding line is devised and aligned to compensate for the antenna inductance.

3. SIMULATION STUDY OF ANTENNA WITH SIMPLIFIED MOBILE PHONE MODEL

A simulation study based on finite difference time domain (FDTD) and finite element method (FEM) analyses was conducted using the SPEAG SEMCAD, 3D full-wave electromagnetic simulation platform.

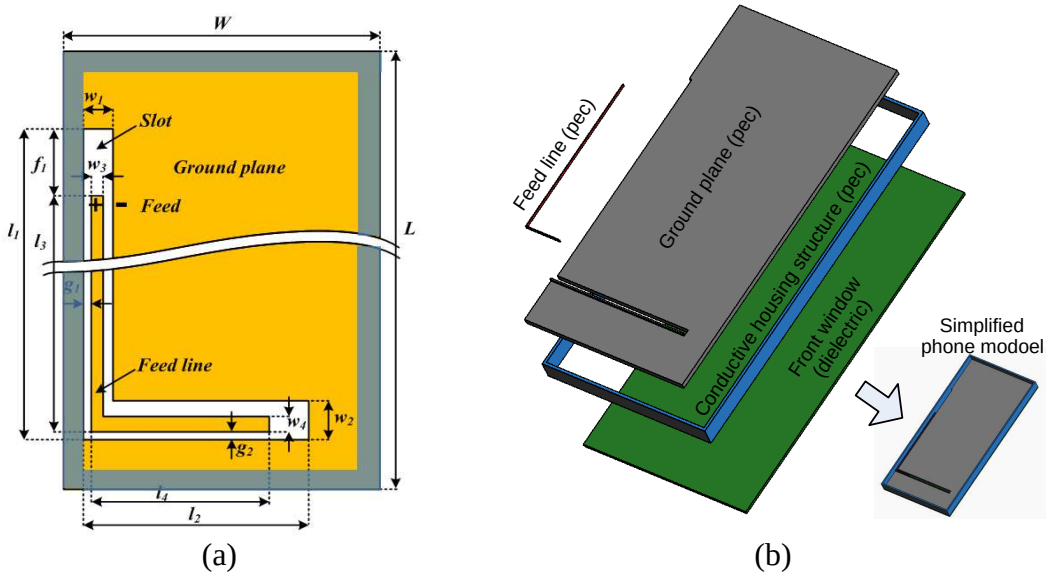

Figure 5. Structural drawings of the proposed slot antenna embedded in mobile phone. (a) Two-dimensional configuration of the proposed antenna. (b) Rear view of the simplified phone metal structure with the proposed antenna.

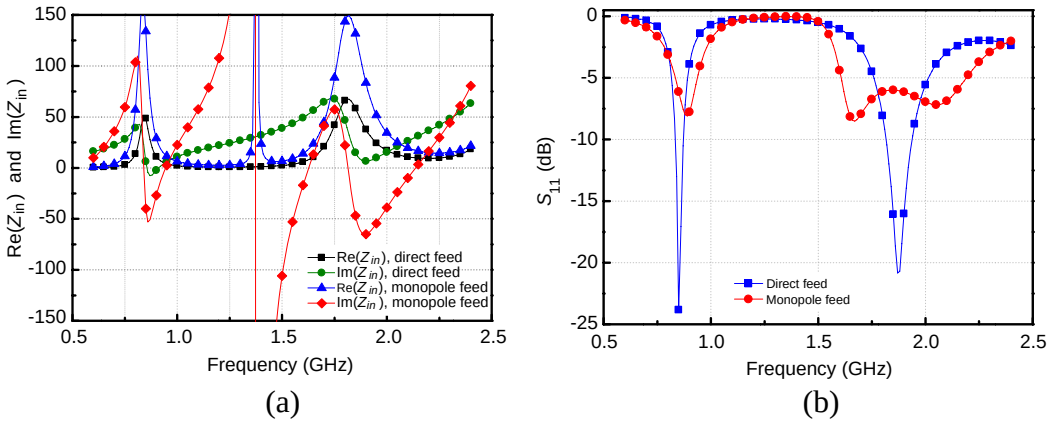

Figure 6. Input impedance and S_{11} of a slot antenna with direct feeding mechanism and a slot antenna with monopole feed line. (a) Input impedance. (b) Return loss

The modeled antenna and the simplified mobile phone assembly with a conductive housing structure are shown in Figure 5(b). The mobile phone consists of a front dielectric window, an LCD bracket, a conductive housing structure (metal frame), and a feed line. Portions of the internal ground plane (LCD bracket) and conductive housing structure form an L-shaped slot antenna of the type shown in Figure 5(a). As a direct feed to this slot antenna cannot provide enough bandwidth to support DCS, PCS, and WCDMA1 operation, an L-shaped feed line is placed along the slot, as illustrated in Figures 5(a) and 5(b), to broaden the bandwidth in the high bands, which for the most part is determined by the location of the feed point and the length of the feed line.

Figure 6 shows the input impedances and return losses of the L-shaped slot antenna, L-shaped feeding line, and direct feeding mechanisms. From this figure, it can be seen that indirect feeding using an L-shaped (slot-tracked) metal line significantly improves the input impedance characteristics in the high bands, enabling the proposed slot antenna design to support the three higher bands (DCS, PCS, and WCDMA1) without relying on additional tuning elements.

Figure 7 shows the current distributions on the ground plane of the conductive housing structures

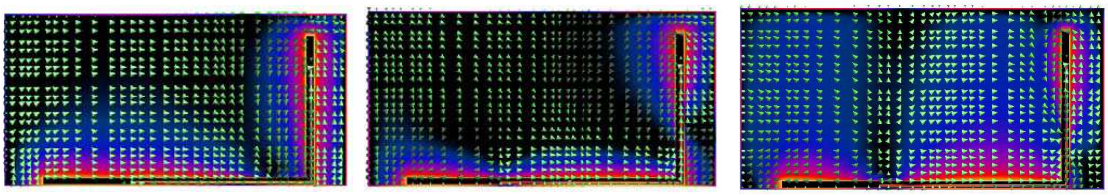

(a) (b) (c)

Figure 7. Current distributions on the ground plane of the proposed antenna. (a) 925 MHz. (b) 1795 MHz. (c) 2045 MHz.

at 925, 1795, and 2045 MHz, which are the central frequencies of the EGSM900, DCS and PCS, and WCDMA1 bands, respectively. The two excited resonant modes correspond to the half and full wavelengths of the resonant structure; at 925 MHz, the slot antenna operates as a half-wavelength resonant structure, while at 1795 and 2045 MHz, it operates as a full-wavelength structure. While the current distribution at the feed point is very strong at 925 MHz, it is reduced at 1795 and 2045 MHz.

3.1. Geometrical Characteristics

In order to provide design guidelines for the model slot antenna-in-phone proposed above, a series of geometrical specifications can be developed based on the dimensions given in Subsection 2.2. Figure 8(a) shows the effects of the slot length on the return loss response for an antenna with $L = 130$, $W = 65$, $l_3 = 70$, $l_4 = 40$, $w_1 = 1$, $w_2 = 2$, $w_3 = 0.2$, $w_4 = 0.2$, $g_1 = 0.2$, and $g_2 = 0.2$ mm (see Figure 5(a)). As the length of the slot (l_1) is increased, f_1 also increases and the first pole of the higher band moves toward lower frequencies, i.e., low band resonance becomes weaker and the first pole of the high band becomes better matched to the source.

The effects of changing the length of the L-shaped feed line at a fixed slot length and $L = 130$, $W = 65$, $l_1 = 95$, $l_2 = 55$, $w_1 = 1$, $w_2 = 2$, $w_3 = 0.2$, $w_4 = 0.2$, $g_1 = 0.2$, and $g_2 = 0.2$ mm are shown in Figure 8(b). Here, the low band response changes very little even when the length of the feed line is increased. On the other hand, the impedance matching characteristics are strongly affected by the length of the feed line; as this increases, the first pole of the high band becomes weaker, while the second pole becomes stronger.

The effects of feed location on return loss at $L = 130$, $W = 65$, $l_1 = 95$, $l_2 = 55$, $w_1 = 1$, $w_2 = 2$, $w_3 = 0.2$, $w_4 = 0.2$, $g_1 = 0.2$, and $g_2 = 0.2$ mm are shown in Figure 8(c). If the feed location is changed while the total length of the feed line remains constant, the dimensions l_4 and f_1 in Figure 5(a) must also change. From Figure 8(c), it can be seen that the feed location has a very small effect on the location of the first pole of the high band, although as the feed approaches one of the slot ends, the low band resonance and the second pole of the high band become strong, while the bandwidth of the high

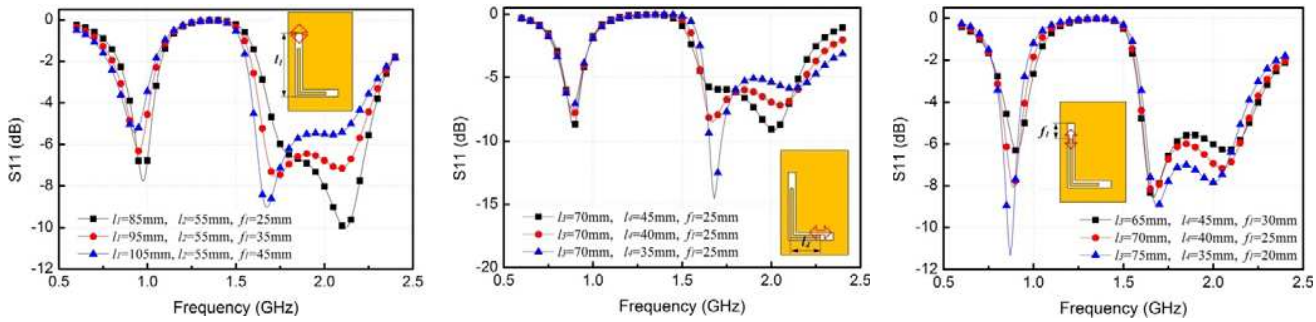

(a) (b) (c)

Figure 8. Geometrical characteristics of the proposed antenna. (a) Effects of the slot length. (b) Effects of the feed line length. (c) Effect of the feed location.

band is reduced slightly.

Based on iterative simulations, optimized dimensions of a proposed, quad-band (EGSM900, DCS, PCS, andWCMA1) antenna were determined, namely: $L = 130$, $W = 65$, $l_1 = 95$, $l_2 = 55$, $l_3 = 70$, $l_4 = 40$, $w_1 = 1$, $w_2 = 2$, $w_3 = 0.2$, $w_4 = 0.2$, $g_1 = 0.2$, $g_2 = 0.2$ and $f_1 = 25$ mm.

4. STUDY WITH MOBILE PHONE

4.1. Implementation

Using the dimensions obtained from the simulation described above, the proposed antenna was incorporated into a real mobile phone. Figure 9 shows the configuration of a prototype mobile phone that includes essential components such as a camera, battery, printed circuit board assembly (PBA), speaker, microphone, and LCD display etc. The slot antenna, which is located between these components and metal enclosures, utilizes the limited mobile phone inner space efficiently, as shown in Figure 9(a). The antenna is embedded in the LCD metal bracket and rectangular loop frame, which is exposed as an exterior decoration; the bracket also serves as the ground plane for the proposed antenna. The assembled prototype like in Figure 9(b) was then passively and actively tested.

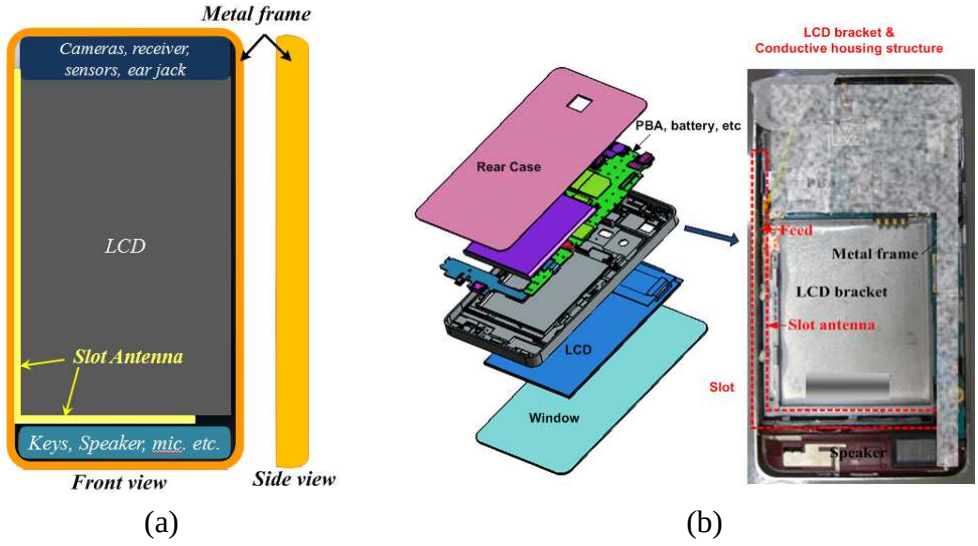

Figure 9. Configuration of the prototype mobile phone with the proposed antenna. (a) Arrangement of the slot antenna. (b) Real phone assembly for simulation and measurement.

4.2. Passive Test Results and Discussion

The return losses obtained using the SPEAG SEMCAD simulation platform are compared with measurements from the antenna-in-phone prototype in Figure 10(a). In the lower bands, there is close agreement between the measured and simulated return losses, but a slight difference occurs in the high bands owing to the complexity of the real mobile phone used for measurement. It is very difficult to make an exact simulation model of a real mobile phone that correctly incorporates all electrical and mechanical components. Based on the 6 dB return loss definition (3 : 1 VSWR) generally used for internal mobile phone antenna design, the measured bandwidth of the lower band is 90 MHz (920–1010 MHz), which allows the antenna to facilitate EGSM900 operation. The bandwidth of the upper band is 530 MHz (1.69–2.22 GHz), which easily satisfies the bandwidth requirements for DCS, PCS, and WCDMA1 operation.

The measured and simulated total radiation efficiencies of the proposed antenna over the four bands are shown in Figure 10(b). Although all of the results closely match, they are not identical owing to a lack of model complexity: the mobile phone used for measurement includes all components and the feeding

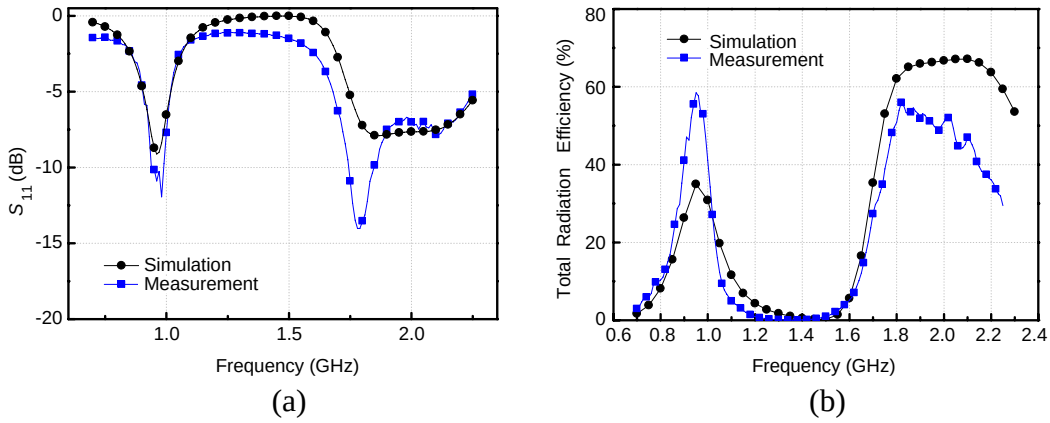

Figure 10. Simulated and measured performances of the proposed antenna in the prototype mobile phone. (a) Return losses. (b) Total radiation efficiencies.

Table 1. The measured total radiation efficiencies of the proposed antenna implemented in the prototype phone.

Band		EGSM900	DCS	PCS	WCDMA1
Tx	Freq. (MHz)	880–915	1910–1785	1850–1910	1920-1980
	Eff. (%)	44.8	39.7	53.3	50.3
Rx	Freq. (MHz)	925–960	1805–1880	1930–1990	2110–2170
	Eff. (%)	57.2	54.2	50.0	40.9

part made by hand soldering, while the simulation model is electrically and mechanically simple. The measured total radiation efficiency within the EGSM900 band varies from 30∼58%, while in the DCS, PCS, and WCDMA1 bands, the measured efficiencies are all above 30%. Averaged radiation efficiencies for these four bands are summarized in Table 1, from which it can be seen that the average efficiency in each band is larger than 40%. This result cannot be obtained through the use of conventional planar inverted F antennas (PIFAs), as these have significantly degraded performance owing to the conductive housing structure in the proximity of the antenna.

4.3. Active Test Results and Discussions

The active performance of an antenna system can be characterized through total radiated power (TRP), total isotropic sensitivity (TIS), and specific absorption rate (SAR) measurements. As TRP and TIS are parts of the Cellular Telecommunication and Internet Association (CTIA) over-the-area (OTA) testing standard, measurements of these can help summarize the performance of a handheld wireless device as an integrated product.

The active radiation performance of the prototype mobile phone was tested in a CTIA-certified anechoic chamber in the low, middle, and high channels of the EGSM900, DCS, PCS, and WCDMA1 bands supported in the prototype; the measured TRPs and TISs under atmospheric conditions are summarized in Table 2. The average TRPs/TISs in the EGSM 900, DCS, PCS, and WCDMA 1 bands are 28.5/−102.7, 27.1/−104.3, 27.5/−103.8, and 21 dBm/−107.3 dBm, respectively, all of which satisfy CTIA requirements and implies that the prototype mobile phone can perform at commercial market standards.

The measured radiation patterns of the proposed antenna in the active condition at 897.4, 1747.6, 1880, and 1950 MHz — which are the central channel frequencies of the EGSM900, DCS, PCS, and WCDMA1 transmitting bands, respectively — are shown in Figure 11. These patterns have a strong visual similarity to that of a monopole antenna, which are often used as conventional mobile phone antennas.

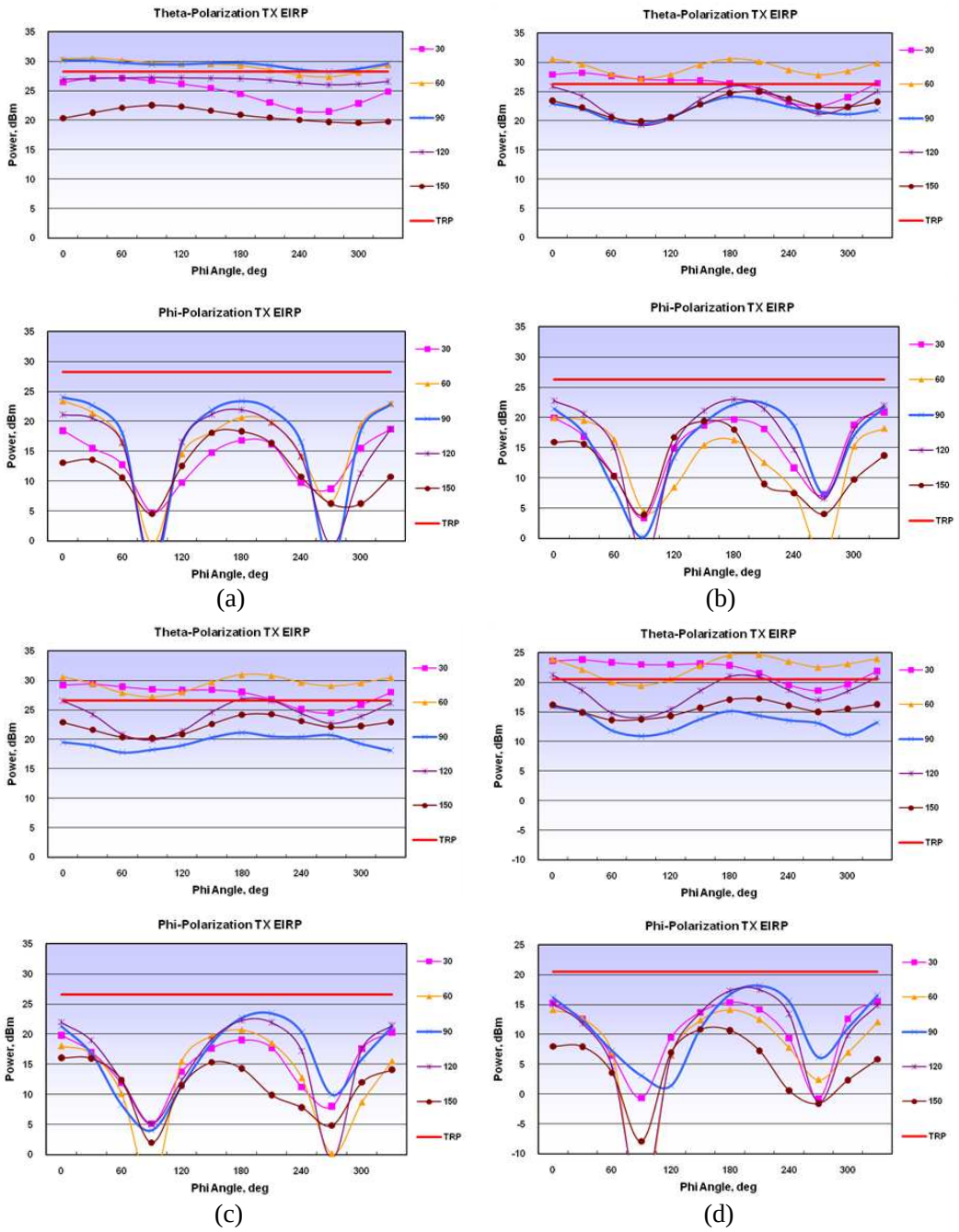

Figure 11. Measured radiation patterns of the proposed antenna embedded in the prototype mobile phone. (a) 897.4 MHz. (b) 1747.6 MHz. (c) 1880 MHz. (d) 1950 MHz.

4.4. Body Effects

The operating environment of a mobile phone affects the radiation properties of its antenna, and the presence of a hand, head, or similar object with high permittivity and large dielectric loss tangent will significantly degrade antenna radiation performance. Figure 12 shows the electric field distribution of the proposed antenna in different situations (with hand, and with hand plus head). From the figure, it is apparent that both the hand and the head distort the large amount of electric field flux passing through them, leading to a high degree of field loss.

Table 2. The measured total radiated powers (TRPs) and total isotropy sensitivities (TISs) of the prototype mobile phone.

Band	Ch. #	TRP (dBm)	TIS (dBm)
EGSM 900	975	28.6	−102.5
	37	28.7	−102.6
	124	28.2	−103.0
DCS	512	27.7	−104.9
	698	27.3	−104.0
	885	26.4	−103.9
PCS	512	27.6	−104.9
	661	27.6	−104
	810	27.3	−102.6
WCDMA1	9613	21.3	−107.2
	9750	21.5	−107.3
	9887	20.3	−107.4

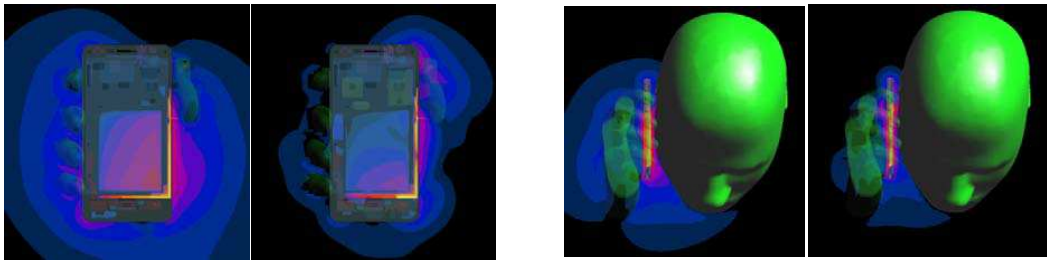

(a) (b)

Figure 12. Simulated electric field of the prototype phone at 898 (left figures of (a) and (b)) and 1748 MHz (right figures of (a) and (b)), the transmitting center frequencies of the GSM900 and DCS band, respectively.

In talking through a mobile phone, the phone will be placed very close to both the hand and head of the user, as shown in Figure 12(b), and this will affect call quality. Phantom body parts were used to measure the TRPs and TISs of the prototype mobile phone in the hand and head condition in the EGSM900, DCS, and WCDMA1 bands, and these measurements were compared to corresponding free space measurements. Changes in the TRPs and TISs owing to the hand and head condition are given in Table 3, which shows measured average losses relative to the free space condition of approximately 6.0, 7.3, and 8.6 dB, respectively, in the EGSM900, DCS, and WCDMA1 bands. Within the EGM900 band, the total loss caused by the hand and head condition is 2∼3 dB, which is better than that occurring in conventional mobile phone PIFAs, while the total loss in the higher band is 1∼2 dB, which is worse than that seen in conventional PIFAs.

Another important test with significant ramifications for antenna and handset design is the measurement of specific absorption rate (SAR), which is driven by an FCC standard that regulates the amount of power that can be absorbed by the human body owing to radio wave exposure. Factors that affect energy absorption by a human body include the size and shape of the device, the distance of the device from the body, the transmitted power level, and the electric current distribution on the device.

The SARs of the prototype mobile phone were calculated using the DASY4 measurement system for the EGSM900, DCS, PCS, and WCDMA1 bands on both the left- and the right-hand sides of the

Table 3. The TRPs and TISs of the prototype phone under hand plus head condition and delta between free space and hand plus head conditions.

(a) EGMS900

	Ch.	Freq.	Free	$H+H$	Delta
TRP	975	880.2	28.6	23.6	**5.0**
	38	897.6	28.7	23.0	**5.7**
	124	914.8	28.2	22.0	**6.2**
TIS	975	925.2	−102.5	−96.6	**5.9**
	38	942.6	−102.6	−95.8	**6.8**
	124	959.8	−103.0	−96.5	**6.5**

(b) DCS

	Ch.	Freq.	Free	$H+H$	Delta
TRP	512	1710.2	27.7	20.0	**7.7**
	701	1748.0	27.3	19.6	**7.7**
	885	1784.8	26.4	19.1	**7.3**
TIS	512	1805.2	−104.9	−97.8	**7.1**
	701	1843.0	−104.0	−97.6	**6.4**
	885	1879.8	−103.9	−96.5	**7.4**

(c) WCDMA1

	Ch.	Freq.	Free	$H+H$	Delta
TRP	9613	1922.8	21.3	11.7	**9.6**
	9750	1950.0	21.5	11.8	**9.7**
	9887	1977.6	20.3	11.3	**9.0**
TIS	9613	2112.4	−107.2	−99.4	**7.8**
	9750	2140.0	−107.3	−99.6	**7.7**
	9887	2167.6	−107.4	−99.4	**8.0**

Table 4. SARs of the prototype phone at the EGSM900, DCS, PCS and WCDMA1 band for both left and right sides of the head.

Band	Ch. #	Freq.	SAR (10 g) [watt/kg]	
			Left	Right
EGSM900	975	880.2	-	1.13
	37	897.4	0.68	0.97
	124	914.8	-	0.79
DCS	512	1710.2	-	0.63
	698	1747.6	0.50	0.60
	885	1784.8	-	0.61
PCS	512	1850.2	-	0.59
	661	1880	0.43	0.59
	810	1909.8	-	0.52
WCDMA	9613	1922.8	-	0.71
	9750	1950.0	0.77	1.10
	9887	1977.6	-	0.80

head using the following formula:

$$\text{SAR} = \frac{\sigma E^2}{\rho} \,[\text{watts/kg}] \tag{1}$$

where σ is the electrical conductivity, ρ is the mass density of the simulation liquid used to mimic a human body, and E is the measured internal electric field strength. The measured 10 g averaged spatial peak SARs of the prototype phone are listed in Table 4; here, the SAR values for all bands (EGSM900, DCS, PCS & WCDMA1) are less than 2.0 W/kg, which is the 10 g SAR standard for both the European Union and Japan.

4.5. Field Test

Field tests simulating poor service environments were performed at several sites at which the value of the received signal strength indication (RSSI) was less than −90 dBm. For comparison, the performance of the prototype phone and a phone currently available in the commercial market were tested simultaneously under the same substandard field conditions; the success rates of calling and answering for each are provided in Table 5, while the speaking and listening (mute test) results are given in Table 6. In both the calling/answering and speaking/listening tests, the mobile phones contacted landline phones, and the calling/answering test measured how calls or answers were successfully made or taken, while the speaking/listening test measured voice quality. From the tables, it can be seen that the prototype mobile phone has better calling and answering performance than the standard phone, which corroborates the results in Tables 3 and 4 in which the prototype phone demonstrates superior free space performance.

Table 5. Calling/answering test results of the prototype phone and the original phone.

	Phone prototyped		Original phone	
	Calling	Answering	Calling	Answering
GSM900	97.5%	90.0%	90.0%	52.5%
DCS	57.5%	37.5%	32.5%	30.0%
WCDMA1	92.5%	92.5%	85.0%	67.5%

Table 6. Speaking/listening test results of the fabricated prototype phone and original phone.

	Phone prototyped		Original phone	
	Speaking	Listening	Speaking	Listening
GSM900	8.8%	45.4%	10.0%	39.2%
DCS	6.3%	41.3%	21.3%	33.8%
WCDMA1	51.3%	26.3%	44.4%	23.1%

5. CONCLUSIONS

As the outward appearance of a mobile phone is a key factor in attracting customers, mobile phone designers have been attempting to develop thinner structures using conductive housing, although their efforts have been hampered by substandard radiation performance. In this paper, a new slot antenna that provides superior radiation performance in conjunction with a surrounding conductive housing structure was proposed. Through extensive simulation and measurement, the performance of this novel antenna system was demonstrated and validated.

ACKNOWLEDGMENT

I would like to express my sincere gratitude to my laboratory mate Jeehoon Lee and former colleagues, Jinkyu Bang, Kyungmoon Seol, Haeyeon Kim, Hoon Park who have readily assisted in all simulations and measurements. This work was supported by the National Research Foundation of Korea (NRF) grant funded by the Korea government (MSIP) (No. 2013014518).

REFERENCES

1. Wong, K. L., *Planar Antennas for Wireless Communications,* Chapter 2, Wiley, New York, 2003.
2. Lindberg, P., E. Ojefors, and A. Rydberg, "Wideband slot antenna for low-profile hand-held terminal application," *Proceeding of the European Conference on Wireless Technology*, 403–406, Sep. 2006.
3. Wong, K.-L., Y.-W. Chi, and S.-Y. Tu, "Printed folded slot antenna for internal multiband mobile phone antenna," *IEEE Antennas and Propagation Society International Symposium*, 2622–2625, Honolulu, HI, Jun. 9–15, 2007.
4. Wong, K.-L., Y.-W. Chi, and S.-Y. Tu, "Internal multiband printed folded slot antenna for mobile phone application," *Microwave and Optical Technology Letters*, Vol. 49, No. 8, 1833–1837, Aug. 2007.
5. Wu, C.-H. and K.-L. Wong, "Internal shorted planar monopole antenna embedded with a resonant spiral slot for penta-band mobile application," *Microwave and Optical Technology Letters*, Vol. 50, No. 52, 529–536, Feb. 2008.
6. Wu, C.-H. and K.-L. Wong, "Hex-band internal printed slot antenna for mobile phone application," *Microwave and Optical Technology Letters*, Vol. 50, No. 1, 35–38, Jan. 2008.
7. Chu, F.-H. and K.-L. Wong, "Simple folded monopole slot antenna for penta-band clamshell mobile phone application," *IEEE Transactions on Antennas and Propagation*, Vol. 57, No. 11, 3680–3684, Nov. 2009.
8. Lin, C.-I. and K.-L. Wong, "Internal hybrid antenna for multiband operation in the mobile phone," *Microwave and Optical Technology Letters*, Vol. 50, No. 1, 38–42, Jan. 2008.
9. Wu, C.-H. and K.-L. Wong, "Internal hybrid loop/monopole slot antenna for quad-band operation in the mobile phone," *Microwave and Optical Technology Letters*, Vol. 50, No. 3, 795—801, Mar. 2008.
10. Rhyu, H., J. Byun, F. J. Harackiewicz, M.-J. Park, K. Jung, D. Kim, N. Kim, T. Kim, and B. Lee, "Multi-band hybrid antenna for untra-thin mobile phone application," *Electronics Letters*, Vol. 45, No. 15, 773–774, Jul. 16, 2009.
11. Sze, J.-Y. and Y.-F. Wu, "A compact planar hexa-band internal antenna for mobile phone," *Progress In Electromagnetics Research*, Vol. 107, 413–425, 2010.